

Alma Mater Studiorum Università di Bologna
Archivio istituzionale della ricerca

Fast hydrogen sorption from MgH₂-VO₂(B) composite materials

This is the final peer-reviewed author's accepted manuscript (postprint) of the following publication:

Published Version:

Fast hydrogen sorption from MgH₂-VO₂(B) composite materials / Milošević, Sanja; Kurko, Sandra; Pasquini, Luca; Matović, Ljiljana; Vujasin, Radojka; Novaković, Nikola; Novaković, Jasmina Grbović. - In: JOURNAL OF POWER SOURCES. - ISSN 0378-7753. - STAMPA. - 307:(2016), pp. 481-488. [10.1016/j.jpowsour.2015.12.108]

Availability:

This version is available at: <https://hdl.handle.net/11585/586705> since: 2017-05-15

Published:

DOI: <http://doi.org/10.1016/j.jpowsour.2015.12.108>

Terms of use:

Some rights reserved. The terms and conditions for the reuse of this version of the manuscript are specified in the publishing policy. For all terms of use and more information see the publisher's website.

This item was downloaded from IRIS Università di Bologna (<https://cris.unibo.it/>).
When citing, please refer to the published version.

(Article begins on next page)

This is the final peer-reviewed accepted manuscript of:

Sanja Milosevic, Sandra Kurko, Luca Pasquini, Ljiljana Matovic, Radojka Vujasin, Nikola Novakovic, Jasmina Grbovic Novakovic, Fast hydrogen sorption from MgH₂–VO₂(B) composite materials, *Journal of Power Sources*, 2016, Volume 307, Pages 481-488.

The final published version is available online at:
<https://doi.org/10.1016/j.jpowsour.2015.12.108>

Rights / License:

The terms and conditions for the reuse of this version of the manuscript are specified in the publishing policy. For all terms of use and more information see the publisher's website.

This item was downloaded from IRIS Università di Bologna (<https://cris.unibo.it/>)

When citing, please refer to the published version.

Fast hydrogen sorption from MgH₂-VO₂(B) composite materials

Sanja Milošević¹, Sandra Kurko¹, Luca Pasquini², Ljiljana Matović¹, Radojka Vujasin¹, Nikola Novaković¹, Jasmina Grbović Novaković¹

¹*Vinča Institute of Nuclear Sciences, University of Belgrade, POB 522, 11000 Belgrade, Serbia*

²*Department of Physics and Astronomy, University of Bologna, v.le Berti Pichat 6/2, I-40127 Bologna, Italy*

ABSTRACT

The hydrogen sorption kinetics of MgH₂-VO₂(B) composites synthesised by mechanical milling have been studied. The microstructural properties of composites were characterized by means of X-ray diffraction (XRD), Raman spectroscopy, Scanning electron microscopy (SEM), Particle size analysis (PSD), while sorption behaviour was followed by differential scanning calorimetry (DSC) and Sievert measurements. Results have shown that although desorption temperature reduction is moderate; there is a substantial improvement in hydrogen sorption kinetics. The complete desorption of pure MgH₂ at elevated temperature takes place in more than 30 minutes while the composite fully desorbs in less than 2 minutes even at lower temperatures. It has been shown that the metastable γ -MgH₂ phase and the point defects have a decisive role in desorption process only in the first sorption cycle, while the second and the subsequent sorption cycles are affected by microstructural and morphological characteristics of the composite.

¹ Jasmina Grbović Novaković, Vinča Institute of Nuclear Sciences, Department of Materials Science, University of Belgrade, POB 522 Belgrade 11000, Serbia, jasnag@vinca.rs, phone: +381 11 3408 552, fax: +381 11 3408 224

Keywords: MgH_2 , $\text{VO}_2(\text{B})$, composites, ball milling, kinetics, desorption

1. INTRODUCTION

Regarding the fact that world-wide use of fossil fuels brings series of ecological problems as well as economy dependence hydrogen energy emerges as viable and sustainable alternative, in a sense of abundance, availability and price. As one of the main problems in hydrogen economy is hydrogen storage and since nowadays known materials for solid-state storage cannot fulfil the targets for automotive applications, fundamental research is needed in this area. Much effort has been devoted to study metal hydrides as materials for hydrogen storage. Metallic magnesium and magnesium based compounds are considered as the most promising candidates. Magnesium is abundant, cheap and a light metal with high gravimetric hydrogen capacity (7.66 wt.%) [1]. Still, high sorption temperature and slow kinetics are main drawbacks of this material.

It has been proven that high energy ball milling of magnesium hydride with various additives (oxide, non-oxide ceramics, amines etc.) improves the hydrogen sorption by reducing particle size and therefore decreasing the desorption temperature at given operating conditions [2–4]. In contrast to hydrides with large particles, the fine powder with its high specific surface area favours hydrogen diffusion and nucleation of MgH_2/Mg [5]. Regarding additives, metal oxides are both catalysts and very efficient milling reagent which, together with milling process, can create desirable changes in magnesium hydride structure such as crystal defects, lattice distortion, increase of specific surface area, increase of active sorption sites density and reduction of the effective diffusion length for sorption (by decrease of the average inter-particle

distance) [6]. A wide range of different metal oxides were used to improve the sorption properties of MgH₂ [7–14]. *Borgschulte et al.* proposed that the oxides present at the interfaces may locally destabilize the magnesium hydride phase [8]. Further, *Oelerich et al.* showed that the highest desorption rates are achieved using V₂O₅ and Fe₃O₄ [9]. Metal oxides are dispersed homogeneously due to their brittleness in a way that can improve desorption properties [2]. In addition, oxide additives reduce apparent activation energy and accelerate the reaction in general [7,9,11–13]. The most favourable effect on desorption temperature was reported by *Aguey-Zinsou et al.* [10]. They used Nb₂O₅, (described as a lubricant, dispersing and cracking reagent) and obtained a shift of DSC maximum from 414°C to 264°C, although amount of additive was relatively high (17 wt.%) and the sample was milled for 200 hours.

Ma et al. [11] investigated dependence of apparent activation energy E_a^{des} for hydrogen desorption on milling time in MgH₂-1mol% Nb₂O₅. They showed that E_a^{des} decreases with the increase of milling time: for 0.02h of milling E_a^{des} = 147 kJmol⁻¹ H₂ while for 20h of milling E_a^{des} = 63 kJmol⁻¹ H₂. *Croston et al.* [12] examined the influence of TiO₂ on desorption properties of MgH₂ and report the reduction of temperature onset from 360°C to 257°C and the reduction of the apparent activation energy to E_d^{des} = 72 ± 3 kJmol⁻¹. Another remarkable reduction of the apparent activation energy for desorption of hydrogen from MgH₂ was reported by *Li et al.* [13]. They used 7mol% of MnFe₂O₄ as a dopant and reported a reduction from 255 kJmol⁻¹ to 65 kJmol⁻¹. Similar effect was reported for CeO₂ addition. The authors obtained apparent activation energy for desorption of E_d^{des} = 60 ± 10 kJmol⁻¹ [7].

Having in mind the fact that catalytic activity of transition-metal compounds can be correlated to several factors, starting from high number of structural defects and valence state of

the transition metal to affinity of the transition metal to hydrogen and low stability of the compound, in this paper we have used VO₂(B), characterised by both vacant structure and high valence state to enhance kinetics of MgH₂ [15,16].

2.EXPERIMENTAL DETAILS

Composites were synthesized by high-energy ball milling process, using Spex 8000M mixer mill with different VO₂(B) quantity (5 and 15 wt. %). VO₂(B) was hydrothermally synthesized starting from V₂O₅, (Merck) [17] as a precursor, while MgH₂ was obtained from Alfa Aesar (98% purity). Composites were milled for 2h using 10:1 ball to powder ratio. All samples were kept and handled in the Ar atmosphere in a glove box. Microstructure, phase composition and morphology of the samples were characterized by X-ray Diffraction (XRD, Panalytical X'Celerator θ - θ diffractometer with filtered Cu-K α radiation), Scanning Electron Microscopy (SEM, JEOL JSM 6460LV) and particle size analysis. To evaluate the average lattice parameters, crystallite size and the relative amount of the different phases before and after cycling, Rietveld analysis of the XRD patterns was carried out using MAUD package [18]. Raman spectra were excited by 514.5nm line of an argon laser and measured at room temperature using a Jobin Yvon model T64000 monochromator, with a CCD detector. Typical resolution was 2cm⁻¹.

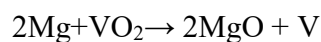
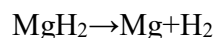
Hydrogen sorption properties were examined using Differential Scanning Calorimetry (DSC) and Sievert's measurements. DSC measurements were performed by TA instrument DSC Q10P in hydrogen flowing environment using 10K/min heating rate in temperature range from 80 to 500°C. The samples were submitted to repeated hydrogen absorption/desorption cycles in a Sievert type apparatus under isothermal conditions in temperature range 330–360°C and pressure

from 0.4–1 bar for desorption and 8–15 bar for absorption keeping the thermodynamic driving force constant according to the formulation of *Rudman et al.* [19].

3.RESULTS AND DISSCUSSION

XRD profiles of both composites obtained by mechanosynthesis with different quantity (5 and 15 wt.%) of VO₂(B) are presented in Figure 1a. The samples are labelled as MV5 and MV15, respectively. The XRD profile both composite after cycling in Sievert's apparatus (entitled as MV15ac) is also presented in Figure 1b. The broad peaks corresponding to β-MgH₂ tetragonal structure are observed in all composites as a result of milling and consequent crystallite size reduction (see Table 1). The XRD profiles show the presence of VO₂(B) as well as reflections attributed to metastable γ-MgH₂ and MgO that were obtained after milling. Formation of γ-MgH₂ and MgO phases is very common after ball-milling [3,6,7,10].

As shown in Table 1, the quantity of MgO in cycled samples is about 46%. This finding suggests that oxidation arises from both, high-temperature reaction with oxygen impurities physisorbed on the samples during handling [6, 7] and from the reactions:



An increase of MgO quantity due to reaction with vanadium oxides has been already reported by several authors [20,21]. The interaction of V with H₂ may lead to formation of an interstitial solid solution, of VH_{~0.8}, or of VH₂ depending on the operating temperature and pressures. At the conditions of our H-sorption cycles, an interstitial solid solution of H in bcc V is expected according to V-H thermodynamics [5]. However, cooling down to room temperature under H₂ results in the successive formation of VH_{~0.8} and VH₂, when the temperature decreases below the dissociation temperature of these hydrides at the actual H₂ pressure.

In fact, XRD patterns after cycling confirmed the formation of VH_2 phase in both samples. One can notice from Figure 1b that MgH_2 , MgO , and VH_2 phases (with some Mg traces in MV5 sample) are present. Some of the Bragg reflections of VH_2 and MgO overlap (see Figure 1b) as the two cubic phases have similar lattice parameters. The intensity of the broad reflection centred at $2\theta \sim 36.8^\circ$ is too high, compared to the MgO (200) reflection centred at $2\theta \sim 42.7^\circ$, to be assigned exclusively to MgO (111) and it originates also from the most intense (111) reflection of VH_2 . The lattice parameter of VH_2 was determined as 4.205(5) Å. Accurate Rietveld refinement permitted to determine the contribution of the two phases to the XRD patterns and to derive the relative phase fractions, which are reported in Table 1.

The XRD profile of MV15ac indicates that after sorption cycling there is a conversion of metastable $\gamma\text{-MgH}_2$ to stable $\beta\text{-MgH}_2$ phase, in accordance with literature data [3, 6]. It is well known that due to the presence of $\gamma\text{-MgH}_2$ in the first desorption cycle there is an appearance of a low temperature DSC peak [3]. In tested samples on the other hand, XRD pattern after cycling does not reveal presence of this metastable phase, so one has to disregard $\gamma\text{-MgH}_2$ phase in practical applications.

Further, since the lattice parameters and c/a ratio of commercial MgH_2 [4] and of composites before and after cycling are very similar [4], no incorporation of V-atom into MgH_2 lattice is expected. Quite interesting is the fact that in the case of MV5 sample, the most of the $\text{VO}_2(\text{B})$ is transformed into VH_2 . On the other hand in MV15 sample, $\text{VO}_2(\text{B})$ has been partially transformed to VH_2 (see Table 1). Nevertheless, the presence of $\text{VO}_2(\text{B})$ after cycling is not detected by XRD analysis, meaning that the quantity of this phase is low and/or the crystallite size is very small.

To gain further information on the V-containing phases after cycling, we employ Raman spectroscopy, which can provide details of short range ordering since it is sensitive to the degree of crystallinity [22].

Raman spectra of hydrothermally synthesized VO₂(B), commercial MgH₂ [23] and MV15ac are shown in Figure 2. The Raman phonon vibrations of VO₂(B) obtained in this study are quite similar to those reported by *Ni et al.* [24] (see Table 2). However, the spectrum in Figure 2 shows only five of eighteen possible Raman bands for low temperature VO₂(B) polymorph. Full spectrum, on the other hand, can be obtained for thin films or for a single crystal [25–28]. The Raman shift of VO₂ bands at 160 cm⁻¹ and 272 cm⁻¹ can be assigned to V–O–V bending modes and external mode (bending/wagging), respectively [24]. The bands at 523 cm⁻¹ can be attributed to V–O–V stretching mode while the band at 705 cm⁻¹ is due to coordination of vanadium atoms with three oxygen atoms. The band at 1015 cm⁻¹ is attributed to V=O stretching of distorted octahedral and distorted square-pyramids [24,29,30].

Regarding composite material MV15ac, one can notice that the whole spectrum exhibits broader features i.e. the bands are wider and the intensity is lower. The sharp band at 311 cm⁻¹ related to MgH₂ Raman active-phonons B_{1g} [23,31] disappears after ball milling and cycling treatment, while a band at 374 cm⁻¹ appears. Several authors reported the VO₂ Raman scattering mode around 390 cm⁻¹. If one takes into account that mechanical milling causes a change in crystal lattice parameters, and therefore a slight shift in position and significant broadening of bands [31–33], the band at 374 cm⁻¹ can be assigned to A_g Raman active-phonon of VO₂.

Due to milling and cycling, the strong and sharp E_g Raman active-phonon at 953 cm⁻¹ of MgH₂ sample is shifted toward lower values (922cm⁻¹, see composite sample). This band is wide and with low intensity. It is interesting to note that the band at 1270 cm⁻¹, which exists in

commercial MgH_2 [23, 34], completely disappears after cycling and milling. Since bands at higher frequencies are related to H-H interactions, one can conclude that this interaction is rather weak after cycling. On the other hand, the low-frequency mode at 120 cm^{-1} [34, 35] related to Mg vibration still exists in the composite sample. Further, the Raman band that corresponds to V–O–V stretching mode (see VO_2 signal, 523 cm^{-1}) is shifted to 542 cm^{-1} in composite material, due to sample milling and interaction with hydrogen during cycling. The VO_2 (B) Raman active mode at 271 cm^{-1} is shifted to 254 cm^{-1} .

Based on the above arguments, Raman analysis suggests that $\text{VO}_2(\text{B})$ is still present in sample MV15 after cycling, i.e. that only partial reduction of $\text{VO}_2(\text{B})$ occurs. In sample MV5, Rietveld analysis implies that VO_2 (B) reduction may be more relevant, but quantitative analysis is difficult due to the low fraction of V-containing phases in this sample.

The composites with different $\text{VO}_2(\text{B})$ amount exhibit a similar morphology, as demonstrated by the SEM micrographs in Figure 3. In both samples, very small particles (less than $2\mu\text{m}$ in size) as well as larger agglomerates (more than $50\mu\text{m}$ in size) are observed, typical for ball-milled powders [5,36]. Particle size distribution (PSD) (see insets in Figure 3) demonstrates a polymodal distribution for both composites in the range of $0.6\text{-}100\mu\text{m}$. 30% of particles have a size smaller than $10\mu\text{m}$, while 70% of particles have size ranging from 10 to $100\mu\text{m}$ in sample MV5. Regarding sample MV15, 27% of particles have size ranging from $0.6\text{-}8\mu\text{m}$, 70% of particles from 8 to $80\mu\text{m}$ and 3% of particles between $80\text{-}100\mu\text{m}$. The changed morphology and reduced particle size have positive effect on sorption properties, as it will be shown later.

Thermal analysis performed by DSC is shown in Figure 4. The endothermic signals of composites, associated with hydrogen desorption, clearly develop in a lower temperature range

with respect to commercial MgH_2 . DSC trace of MV5 exhibits two broad peaks at $\sim 395^\circ\text{C}$ and $\sim 420^\circ\text{C}$, while MV15 is characterized by a maximum at $\sim 400^\circ\text{C}$ with strong asymmetry towards higher temperatures. These features suggest that hydrogen desorption occurs as two steps process. One can argue that the bimodal particle size distribution is one of the reasons for such DSC behaviour. On the other hand, as shown by XRD, the presence of $\gamma\text{-MgH}_2$ in composites after milling cannot be excluded as a possible reason of two DSC maxima. Similar temperatures for hydrogen desorption during DSC scans are reported in the literature for different MgH_2 -based composites [36,37]. The area under the endothermic desorption peak in the DSC traces decreases from 1380Jg^{-1} for commercial MgH_2 to about 1200Jg^{-1} for the composites. Such reduction reflects a decrease of the overall gravimetric hydrogen storage capacities of the composites, due to a presence of vanadium based compounds and formation of MgO .

The Sievert's apparatus was used to record hydrogen sorption kinetics under isothermal conditions. In the commercial MgH_2 , at temperature of 380°C and pressure of 1bar, the hydrogen desorption capacity saturates at 6.9 wt.% in about 30 min (Figure 5a). At lower temperature ($350^\circ\text{C}/0.7\text{bar}$), hydrogen desorption process is significantly slower, reaching only 2.9 wt.% in 5000 min (Figure 5a).

As it can be seen in Figure 5a, composite MV5 shows significant acceleration of hydrogen desorption: at $350^\circ\text{C}/1\text{bar}$ capacity of 4.9 wt.% is reached after ~ 120 seconds, while composite MV15 reaches the capacity of 4.3wt.% after 85 seconds at $350^\circ\text{C}/0.7\text{bar}$. Similar improvement was reported by *Grigorova et al.* [38] for composites with vanadium in valence state 5 (capacity of 5.4% after 25 minutes at 350°C) and *Khrussanova et al.* [39] from $90\%\text{Mg}+10\%\text{V}_2\text{O}_5$ ($\sim 4.3\%$ after 30 minutes and the activation energy of 89.7kJmol^{-1}). It is worth noticing that all these observations are valid for the first desorption cycle.

Desorption curves in Figure 5a and 5b show the difference between the first and all subsequent desorption cycles. One can argue that the second and subsequent cycles are affected by chemical composition (type of matrix and catalyst), microstructural and morphological characteristics of composite (particle size of matrix and the catalyst, distribution of the catalyst). Induced vacancies and introduced defects in crystal lattice affect only the first desorption cycle [40]. After subsequent sorption, the material relaxes, so the vacancies and defects disappear and their influence on desorption is negligible. Therefore the activation process has been followed in details. Figure 6 shows sorption cycling of MV15 composite at 320°C before "activation"² and after activation at 380°C. Comparing the storage capacities, one can notice that the capacity without activation process is lower (4.3 wt.%, 4.8 wt.%, 5.0 wt.% in 1st, 2nd and 3rd desorption, respectively) and gradually increases with cycling. After activation, one can see that the hydrogen desorption capacity attains a higher value of 5.4 wt.%, which remains constant during subsequent cycles. Korablov et al. spotted similar behaviour after cycling of MgH₂-V₂O₅ system and correlate it to the *in situ* formation of VH₂/V in the sample [20]. In fact, in the system MgH₂-VO₂, Raman and XRD analysis shows formation of VH₂ upon cycling and therefore the existence of VO₂/VH₂ (V⁴⁺/V²⁺) system is probably responsible for strongly improved (de)sorption kinetics. Regarding the mechanism of kinetic reaction one can argue that the existence of multivalent V acts as an intermediate between Mg²⁺ and H⁻. Indeed, based on XPS analysis Cui et al. [41] proposed similar mechanism for addition of Ti based compounds to MgH₂. They have found that the interfaces between high valence and low valence Ti compounds are actually responsible for improved kinetics by favoring electron transfer between Mg²⁺ and H⁻ at the interface and proposed following three-step mechanism: 1) at the hydride/metal interface, H⁻

² Activation process: uptake and release of hydrogen at elevated temperature

donates an electron to high valence V, which transforms into low valence V; 2) e^- transfer weakens Mg–H bonds and dissociated H is formed, leading to dehydrogenation; 3) finally, two H atoms recombine to form one H_2 molecule, while the metallic Mg phase nucleates and grows.

Recently Paskaš Mamula et al [42] showed using DFT calculations that the substitution of Mg with 3d transition metals results in weaker Mg-H bonds and shorter and stronger TM-H bonds. Further, they have revealed that Bader charge analysis [42] (number, distribution and charge of bonding critical points and attraction basin integrated charges) goes in favor of more directional bonding with larger share of covalence. One must have in mind that the effect is quite localized and constrained to several coordination shells. They have shown that V-H bonds are slightly shorter (1.845 Å) compared to 1.959 Å in pure MgH_2 and are almost the same as in VH_2 (1.85 Å [43]), despite the lower coordination number. The stability of MgH_2 -V system is lowered as a direct consequence of dopant concentration (6.25 at%), meaning that localized changes in host lattice caused by V doping are compensated by its concentration.

Hydrogen sorption kinetic curves were fitted according to the Johnson-Mehl-Avrami (JMA) nucleation and growth model: $f(t) = 1 - \exp[-(kt)^n]$ where f is the transformed fraction as a function of time t , k is the rate constant and n is Avrami exponent (see Figure 7). The kinetic parameters obtained from the best fit are listed in Table 3. The mechanism of phase transformation was determined using the n value and the apparent activation energies [44, 45]. It can be noticed that n values fluctuate around 1.5 for MV5 and 1.9 for MV15 for composites indicating that there is change in the mechanism of desorption regarding dimensionality of nuclei and the nucleation rate [35]. As it can be seen from Table 4 Avrami exponent can adopt different values depending on the parameters. Avrami exponent is given by $n = a + b \cdot c$ where a is determined by the nucleation mechanism and $a = 0$ for an instant nucleation, $0 < a < 1$ for

decreasing nucleation rate, $a = 1$ for constant nucleation rate and $a > 1$ for increasing nucleation rate. On the other hand, b is related to the growth dimensionality ($b = 1, 2$ and 3) and c indicates diffusion-controlled ($c = 0.5$) or interface-controlled ($c = 1$) growth [44, 45]. Therefore, it is difficult to identify the exact mechanism of desorption, but it is obvious that the probability of 2D growth increases with $\text{VO}_2(\text{B})$ addition (see Table 3).

Significant decrease of the apparent activation energies with the addition of catalyst confirms the effectiveness of $\text{VO}_2(\text{B})$, which probably acts as nucleation site for the growth of the transformed phase. The obtained E_A^{des} (using JMA), together with literature data, is listed in Table 5. It can be noticed that the apparent activation energies vary depending on the nature of the catalyst but also on the quantity of added phase. Comparing to the apparent activation energy for desorption of pure MgH_2 (161 kJmol^{-1}) obtained by *Fernandez et al.* [46], it can be noticed that E_A^{des} significantly decreases with the addition of $\text{VO}_2(\text{B})$. Further, our study confirms the findings of *Barkhordarian et al.* [47], who demonstrated that the apparent activation energy varies with the quantity of added phase.

The results obtained by *Kurko et al.* suggest that lower hydrogen coverage of the surface makes diffusion toward the surface easier [48]. *Borgschulte et al.* suggested that due to formation of vacancies the rate-limiting step is not the dissociation by the active sites, but the number as well as the transport to active sites, i.e. the diffusion on/in oxides [49]. On the other hand, DFT calculation performed by *Du et al.* demonstrates that the diffusion of H-vacancy from an in-plane site to a bridge site on the surface has the smallest activation barrier of 0.15 eV and should be fast at room temperature [50]. The calculated activation barriers for H-vacancy diffusion from the surface into sublayers are all less than 0.70 eV , which is much lower than the activation energy for hydrogen desorption at the MgH_2 (110) surface ($1.78\text{-}2.80 \text{ eV/H}_2$) [50]. This suggests

that surface desorption is the rate determining step rather than vacancy diffusion, so finding an effective catalyst is very important for improving the overall dehydrogenation performances of hydrides. Obviously, obtained apparent activation energy for desorption of about 60kJmol^{-1} (0.63 eV) suggests that $\text{VO}_2(\text{B})$ can be used as an excellent catalysts for sorption processes even though the catalytic reaction goes through formation of multivalent system VO_2/VH_2 .

4. CONCLUSIONS

Composites $\text{MgH}_2\text{--VO}_2(\text{B})$ were synthesised by mechanical milling and their hydrogen sorption properties were studied. The broadening of typical peaks corresponding to $\beta\text{--MgH}_2$ tetragonal structure is observed in all composites as a result of milling and consequent crystallite size reduction. The XRD profiles show the presence of $\text{VO}_2(\text{B})$, as well as reflections attributed to metastable $\gamma\text{--MgH}_2$ and MgO . Upon cycling, the metastable phase $\gamma\text{--MgH}_2$ converts into a stable $\beta\text{--MgH}_2$ phase, and the crystalline VH_2 phase appears. Raman spectra confirm the presence of $\text{VO}_2(\text{B})$ phase after cycling in the sample with higher quantity of $\text{VO}_2(\text{B})$, i.e. MV15ac. XRD analysis indicates that part of $\text{VO}_2(\text{B})$ is reduced to V metal at high temperature, with concomitant oxidation of Mg into MgO . Particle size distribution demonstrates polymodal distribution for both composites. There is a shift of desorption temperature toward lower values (about 60°C) and a decrease of gravimetric storage capacity, mainly due to presence of MgO . On the other hand, hydrogen sorption kinetics is substantially improved (from 2.9 wt.% in 5000 min for commercial MgH_2 to 4.9 wt.% in 120 seconds at $350^\circ\text{C}/1\text{bar}$ for MV5 sample) due to presence of multivalent V i.e. VO_2/VH_2 system. A considerable difference between first and subsequent sorption cycles is caused by structure relaxation, structure defects disappearance and the presence of VO_2/VH_2 . The defect structure and number of vacancies seem to play a more

important role than valence state in the first desorption cycle, while the second and subsequent cycles are more likely improved due to presence of VO_2/VH_2 .

ACKNOWLEDGEMENT

This research was financially supported by Ministry of Education, Science and Technology of the Republic of Serbia under grant III 45012. The authors express their gratitude to COST Action MP1103 “Nanostructured Materials for Solid State Hydrogen Storage”. Authors are grateful to Dr Nebojša Romčević from Institute of Physics, University of Belgrade, Serbia for Raman spectra measurements.

REFERENCES

- [1] B. Bogdanović, T.H. Hartwig, B. Spliethoff, The development, testing and optimization of energy storage materials based on the MgH_2 -Mg system, *Int. J. Hydrogen Energy* 18 (1993) 575–589.
- [2] T. Sadhasivam, M. Sterlin Leo Hudson, S.K. Pandey, A. Bhatnagar, M.K. Singh, K. Gurunathan, O.N. Srivastava, Effects of nano size mischmetal and its oxide on improving the hydrogen sorption behaviour of MgH_2 , *Int. J. Hydrogen Energy* 38 (2013) 7353–7362.
- [3] R.A. Varin, T. Czujko, Z. Wronski, Particle size, grain size and γ - MgH_2 effects on the desorption properties of commercial magnesium hydride processed by controlled mechanical milling, *Nanotechnology* 17 (2006) 3856–3865.

- [4] I. Milanović, S. Milošević, Ž. Rašković-Lovre, N. Novaković, R. Vujasin, Lj. Matović, J. Francisco Fernández, C. Sánchez, J. Grbović Novaković, Microstructure and hydrogen storage properties of $\text{MgH}_2\text{-TiB}_2\text{-SiC}$ composites, *Ceram. Int.* 39 (2013) 4399–4405.
- [5] R.A. Varin, T. Czujko, Z.S. Wronski, *Nanomaterials for Solid State Hydrogen Storage*, Springer, New York, 2009.
- [6] A. Bassetti, E. Bonetti, L. Pasquini, A. Montone, J. Grbović, M. Vittori Antisari, Hydrogen desorption from ball milled MgH_2 catalyzed with Fe, *Eur. Phys. J. B* 43 (2005) 19–27.
- [7] J. Gulicovski, Ž. Rašković-Lovre, S. Kurko, R. Vujasin, Z. Jovanović, Lj. Matović, J. Grbović Novaković, Influence of vacant CeO_2 nanostructured ceramics on MgH_2 , *Ceram. Int.* 38(2) (2012) 1181–1186.
- [8] A. Borgschulte, U. Bosenberg, G. Barkhordarian, M. Dornheim, R. Bormann. Enhanced hydrogen sorption kinetics of magnesium by destabilized $\text{MgH}_2\text{-}\beta$, *Catal. Today* 120 (2007) 262–269.
- [9] W. Oelerich, T. Klassen, R. Bormann, Metal oxides as catalysts for improved hydrogen sorption in nanocrystalline Mg-based materials, *J. Alloy. Compd.* 315 (2001) 237–242.
- [10] K.-F. Aguey-Zinsou, J.R. Ares Fernandez, T. Klassen, R. Bormann, Effect of Nb_2O_5 on MgH_2 properties during mechanical milling, *Int. J. Hydrogen Energy* 32 (2007) 2400–2407
- [11] T. Ma, S. Isobe, E. Morita, Y. Wang, N. Hashimoto, S. Ohnuki, T. Kimura, T. Ichikawa, Y. Kojima, Correlation between kinetics and chemical bonding state of catalyst surface in catalyzed magnesium hydride, *Int. J. Hydrogen Energy* 36 (2011) 12319–12323.
- [12] D.L. Croston, D.M. Grant, G.S. Walker, The catalytic effect of titanium oxide based additives on the dehydrogenation and hydrogenation of milled MgH_2 , *J. Alloy. Compd.* 492 (2010) 251–258.

- [13] P. Li, Q. Wan, Z. Li, F. Zhai, Y. Li, L. Cui, X. Qu, A.A. Volinsky, MgH₂ dehydrogenation properties improved by MnFe₂O₄ nanoparticles, *J. Power Sources* 239 (2013) 201–206.
- [14] M.Y. Song, J.-L. Bobet, B. Darriet, Improvement in hydrogen sorption properties of Mg by reactive mechanical grinding with Cr₂O₃, Al₂O₃ and CeO₂, *J. Alloy. Compd.* 340 (2002) 256–262.
- [15] G. Barkhordarian, T. Klassen, R. Bormann, Catalytic Mechanism of Transition-Metal Compounds on Mg Hydrogen Sorption Reaction, *J. Phys. Chem. B* 110(22) (2006) 11020–11024.
- [16] W. Oelerich, T. Klassen, R. Bormann, Comparison of the catalytic effects of V, V₂O₅, VN, and VC on the hydrogen sorption of nanocrystalline Mg, *J. Alloy. Compd.* 322 (2001) L5–L9.
- [17] S. Milošević, I. Stojković, S. Kurko, J. Grbović Novaković, N. Cvjetičanin, The simple one-step solvothermal synthesis of nanostructured VO₂(B), *Ceram. Int.* 38 (2012) 2313–2317.
- [18] L. Lutterotti, P. Scardi, Simultaneous structure and size-strain refinement by the Rietveld method, *J. Appl. Crystallogr.* 23 (1990) 246–252.
- [19] P.S. Rudman. Hydrogen-diffusion-rate-limited hydriding and dehydriding kinetics. *J. Appl. Phys.* 50 (1979) 7195–7199.
- [20] D. Korablov, T.K. Nielsen, F. Besenbacher, T.R. Jensen, Mechanism and kinetics of early transition metal hydrides, oxides, and chlorides to enhance hydrogen release and uptake properties of MgH₂, *Powder Diffr.* 30 (2015) S9–S15.
- [21] D.L. Anton, C.J. Price, J. Gray, Affects of mechanical milling and metal oxide additives on sorption kinetics of 1:1 LiNH₂/MgH₂ mixture, *Energies* 4 (2011) 826–844.

- [22] K. Nakamoto, *Infrared and Raman Spectra of Inorganic and Coordination Compounds: Part A: Theory and Applications in Inorganic Chemistry*, Sixth Ed., A John Wiley & Sons, INC., Publication, New Jersey, 2009.
- [23] Lj. Matovic, N. Novakovic, S. Kurko, M. Siljegovic, B. Matovic, Z. Kacarevic-Popovic, N. Romcevic, N. Ivanovic, J. Grbovic Novakovic, Structural destabilisation of MgH_2 obtained by heavy ion irradiation, *Int. J. Hydrogen Energy* 34 (2009) 7275–7282.
- [24] S. Ni, H. Zeng, X. Yang, Fabrication of $\text{VO}_2(\text{B})$ Nanobelts and Their Application in Lithium Ion Batteries, *J. Nanomaterials* 2011 (2011) Article ID 961389
doi:10.1155/2011/961389.
- [25] E.M. Heckman, L.P. Gonzalez, S. Guha, J.O. Barnes, A. Carpenter, Electrical and optical switching properties of ion implanted VO_2 , *Thin Solid Films* 518 (2009) 265–268.
- [26] X. B Chen, Assignment of the Raman Modes of VO_2 in the Monoclinic Insulating Phase, *J. Korean Phys. Soc.* 58(1) (2011) 100–104.
- [27] R. Srivastava, L.L. Chase, Raman spectrum of Semiconducting and Metallic VO_2 *Phys. Rev. Lett.* 27 (1971) 727–730.
- [28] V.S. Vikhnin, I.N. Goncharuk, V.Y. Davydov, F.A. Chudnovskii, E.B. Shadrin, Raman spectra of the high-temperature phase of vanadium dioxide and model of structural transformations near the metal-semiconductor phase transition *Phys. Solid State* 37 (1995) 1971–1978.
- [29] J. Twu, C.F. Shih, T.H. Guo, K.H. Chen, Raman spectroscopic studies of the thermal decomposition mechanism of ammonium metavanadate, *J. Mater. Chem.* 7(11) (1997) 2273–2277.

- [30] F.D. Hardcastle, I.E. Wachs, Determination of vanadium-oxygen bond distances and bond orders by Raman spectroscopy, *J. Phys Chem.* 95(13) (1991) 5031–5041.
- [31] M. Pan, J. Liu, H. Zhong, S. Wang, Z. Li, X. Chen, W. Lu, Raman study of the phase transition in VO₂ thin films, *J. Cryst. Growth* 268 (2004) 178–183.
- [32] H.G. Schimmel, M.R. Johnson, G.J. Kearley, A.J. Ramirez-Cuesta, J. Huot, F.M. Mulder, Structural information on ball milled magnesium hydride from vibrational spectroscopy and ab-initio calculations, *J. Alloy. Compd.* 393 (2005) 1–4
- [33] F.H. Pollak, in: J.G. Grasselli, B.J. Bulkin (Eds.), *Analytical Raman Spectroscopy*, vol. 167, Wiley & Sons, New York, 1991.
- [34] J. Lasave, F. Dominguez, S. Koval, M.G. Stachiotti, R.L. Migoni, Shell-model description of lattice dynamical properties of MgH₂, *J. Phys.: Condens. Matter.* 17 (2005) 7133–7141.
- [35] J.R. Santisteban, G.J. Cuello, J. Dawidowski, A. Fainstein, H.A. Peretti, A. Ivanov, F.J. Bermejo, Vibrational spectrum of magnesium hydride, *Phys. Rev. B* 62 (2000) 37–40.
- [36] A. Montone, A. Aurora, D. Mirabile Gattia, M. Vittori Antisari, Microstructural and Kinetic Evolution of Fe Doped MgH₂ during H₂ Cycling, *Catalysts* 2 (2012) 400–411.
- [37] J. Bystrzycki, M. Polanski, T. Plocinsk, Nano-engineering approach to destabilization of magnesium hydride (MgH₂) by solid-state reaction with Si, *J. Nanosci. Nanotechnol.* 8 (2008) 1–8.
- [38] E. Grigorova, M. Khristov, P. Peshev, D. Nihtianova, N. Velichkova, G. Atanasova, Hydrogen sorption properties of a MgH₂-V₂O₅ composite prepared by ball milling, *Bulg. Chem. Commun.* 45 (2013) 280–287.
- [39] M. Khrussanova, M. Terzieva, P. Peshev, On the hydriding of a mechanically alloyed Mg(90%)-V₂O₅(10%) mixture, *Int. J. Hydrogen Energy* 15 (1990) 799–805.

- [40] J. Grbović Novaković, Lj. Matović, M. Drvendžija, N. Novaković, D. Rajnović, M. Šiljegović, Z. Kačarević Popović, S. Milovanović, N. Ivanović, Changes of hydrogen storage properties of MgH_2 induced by heavy ion irradiation, *Int. J. Hydrogen Energy* 33 (2008) 1876–1879.
- [41] J. Cui, H. Wang, X. Yao, J. Liu, M. Zhu, L. Ouyang, Q. Zhang, D. Sun, Remarkable enhancement in dehydrogenation of MgH_2 by a nano-coating of multi-valence Ti-based catalysts, *J. Mater. Chem. A* (2013) 5603–5611.
- [42] B. Paskaš Mamula, J. Grbović Novaković, I. Radisavljević, N. Ivanović, N. Novaković, Electronic Structure and Charge Distribution Topology of MgH_2 doped with 3d Transition Metals, *Int. J. Hydrogen Energy* 39(11) (2014) 5874–5887.
- [43] T. Vegge, L.S. Hedegaard-Jensen, J. Bonde, T.R. Munter, J.K. Nørskov, Trends in hydride formation energies for magnesium-3d transition metal alloys, *J. Alloys Compd.* 386 (2005) 1–7.
- [44] A. Montone, A. Aurora, D. Mirabile Gattia, M. Vittori Antisari, Effect of hydrogen pressure and temperature on the reaction kinetics between Fe-doped Mg and hydrogen gas, *J. Alloy. Compd.* 509 (2011) S580–S583.
- [45] A.T.W. Kempen, F. Sommer, E.J. Mittemeijer, Determination and interpretation of isothermal and non-isothermal transformation kinetics; The effective activation energies in terms of nucleation and growth, *J. Mater. Sci.* 37 (2002) 1321–1332.
- [46] J.F. Fernandez, C.R. Sanchez, Simultaneous TDS–DSC measurements in magnesium hydride, *J. Alloy. Compd.* 356–357 (2003) 348–352.
- [47] G. Barkhordarian, T. Klassen, R. Bormann, Effect of Nb_2O_5 content on hydrogen reaction kinetics of Mg, *J. Alloy. Compd.* 364 (2004) 242–246.

- [48] S. Kurko, I. Milanovic, J. Grbovic Novakovic, N. Ivanovic, N. Novakovic, Investigation of surface and near-surface effects on hydrogen desorption kinetics of MgH_2 , *Int. J. Hydrogen Energy* 39(2) (2014) 862–867.
- [49] A. Borgschulte, M. Biemann, A. Züttel, G. Barkhordarian, M. Dornheim, R. Bormann, Hydrogen dissociation on oxide covered MgH_2 by catalytically active vacancies, *Appl. Surf. Sci.* 254 (2008) 2377–2384.
- [50] A.J. Du, S.C. Smith, G.Q. Lu, First-principle studies of the formation and diffusion of hydrogen vacancies in magnesium hydride, *J. Phys. Chem. C* 111(23) (2007) 8360–8365.